Compressive strain measurement using RFID patch antenna sensors

Chunhee Cho [a], Xiaohua Yi [a], Yang Wang [a*], Manos M. Tentzeris [b], and Roberto T. Leon [c]

[a] School of Civil and Environmental Eng., Georgia Inst. of Technology, Atlanta, GA 30332, USA
[b] School of Electrical and Computer Eng., Georgia Inst. of Technology, Atlanta, GA 30332, USA
[c] Department of Civil and Environmental Eng., Virginia Polytechnic Inst. and State Univ., Blacksburg, VA 24061, USA

ABSTRACT

In this research, two radiofrequency identification (RFID) antenna sensor designs are tested for compressive strain measurement. The first design is a passive (battery-free) folded patch antenna sensor with a planar dimension of 61mm × 69mm. The second design is a slotted patch antenna sensor, whose dimension is reduced to 48mm × 44mm by introducing slots on antenna conducting layer to detour surface current path. A three-point bending setup is fabricated to apply compression on a tapered aluminum specimen mounted with an antenna sensor. Mechanics-electromagnetics coupled simulation shows that the antenna resonance frequency shifts when each antenna sensor is under compressive strain. Extensive compression tests are conducted to verify the strain sensing performance of the two sensors. Experimental results confirm that the resonance frequency of each antenna sensor increases in an approximately linear relationship with respect to compressive strain. The compressive strain sensing performance of the two RFID antenna sensors, including strain sensitivity and determination coefficient, is evaluated based on the experimental data.

Keywords: strain sensor, RFID, passive wireless sensor, folded patch antenna, slotted patch antenna

1. INTRODUCTION

In recent decades, structural health monitoring has remained as an important issue for various engineering structures [1]. For example, to measure strain and stress concentration on a structure, many strain sensing technologies have been developed, such as metal foil strain gages, piezoelectric strain sensors, and fiber optic sensors [2, 3]. Although these strain sensors show promising sensing performance, most of them require cables for powering or data acquisition. Cable installation presents difficulty not only in large-scale field instrumentation, but also in long-term maintenance of the monitoring system [4]. Therefore, vast amount of efforts have been made to reduce installation time and cost by developing wireless strain sensing systems. Such systems commonly integrate an analog-to-digital converter for signal digitization, a microprocessor for data processing, and a wireless data transceiver [5-7]. However, these wireless systems usually require external battery power, which limits the life span of the sensor and may cause environmental concerns.

In our previous research, a folded patch antenna sensor and a slotted patch antenna sensor are developed for wireless strain sensing. Both sensors adopt passive (battery-free) RFID (radio frequency identification) technology [8, 9]. During operation, an RFID reader emits interrogation power to the antenna sensor. The power received by the antenna is used to activate the RFID chip, so that the chip modulates RF signal scattered back to the reader. Since electromagnetic resonance frequency of the sensor is dependent on the antenna dimension, the resonance frequency shifts when strain is experienced.

The folded patch antenna configuration reduces the sensor footprint to about half of a normal rectangular patch antenna (i.e. without folding). The tensile strain sensing performance of the folded patch antenna sensor has been validated through extensive simulations and experiments. The strain sensitivity is around –750Hz/με, and the maximum interrogation distance over 2m [8, 10]. The slotted patch antenna sensor footprint is further reduced by adding slots to detour surface current path on the antenna. Despite large size reduction, the slotted patch antenna sensor shows similar tensile strain sensing performance as the folded patch [9]. Nevertheless, although both sensors demonstrate acceptable performance for tensile strain sensing, performance on compressive strain sensing has not been extensively studied.

*yang.wang@ce.gatech.edu; phone 1 (404) 894-1851; fax 1 (404) 894-2278

This paper presents compressive strain sensing performance of the two antenna sensors. In order to conveniently generate uniform compressive strain, a tapered aluminum specimen and a three-point bending setup is designed. The compressive strain sensing performance of both antenna sensors are first simulated using a commercial software package, COMSOL, which supports mechanics-electromagnetics coupled simulation. Extensive compression experiments are then conducted to validate the compressive strain sensing performance. The rest of this paper is organized as follows. Section 2 describes the compressive strain sensing setup and reviews both antenna designs. Section 3 presents multi-physics coupled mechanics-electromagnetics simulation for each sensor. Section 4 discusses laboratory experimental results of both sensors. Finally, the research is summarized with a conclusion and future work.

2. COMPRESSIVE STRAIN SENSING SETUP FOR RFID ANTENNA SENSORS

This section introduces the experimental setup for testing wireless compression sensing performance. Section 2.1 describes the experimental setup to generate compressive strain on the antenna sensor. Section 2.2 and 2.3 briefly review the folded and slotted antenna sensor designs, respectively [9, 11].

2.1 A three-point bending device designed for compressive strain testing

For characterizing compression sensing performance, an antenna sensor needs to be first bonded to the surface of a test specimen. The sensor can experience compression together with the specimen. Although uniform compressive strain can be directly generated by applying axial force to a test specimen, the specimen would need to be a stocky column to avoid buckling. The approach also requires an expensive high capacity compressive testing machine. Therefore, a three-point bending compression setup is fabricated as an alternative approach to generate compressive strain, as shown in Fig. 1. While the specimen is held in the middle by strong fixtures, two screw bolts (one at each end of the specimen) are adjusted to generate bending in the specimen. This in effect produces compressive strain on the specimen surface. Because surface compressive strain is not uniform along axial direction when a rectangular-shaped plate experiences three-point bending, a tapered aluminum specimen (AL6061) is designed to generate approximately uniform strain (Fig. 2).

Fig. 1 also illustrates the wireless strain sensing system, including a reader and an antenna sensor. During operation, the reader first emits interrogation electromagnetic signal to the antenna sensor. If the sensor is in the interrogation range of
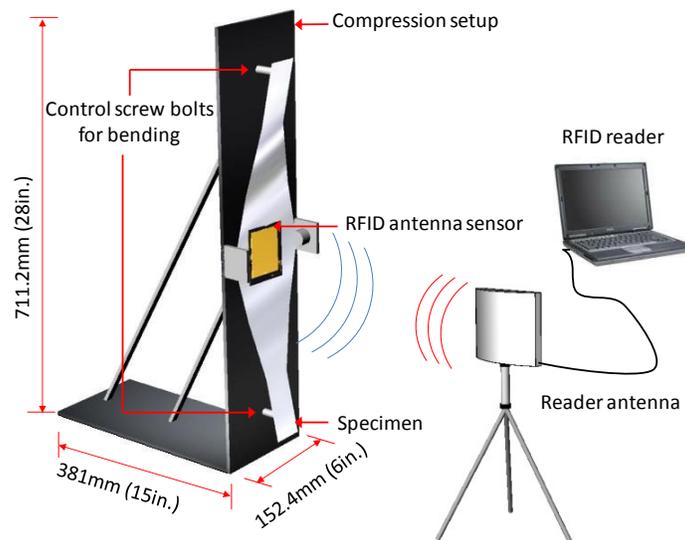

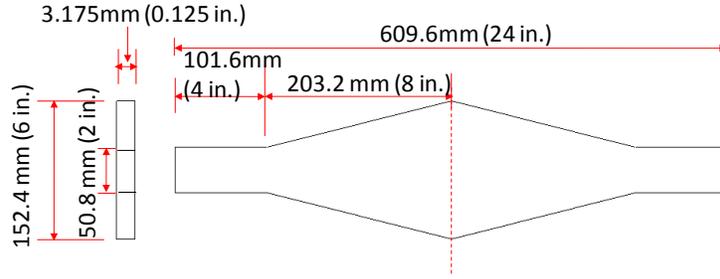Fig. 1. Conceptual illustration of compressive strain sensing mechanism

Fig. 2. Dimension of a tapered aluminum specimen for compression test

the reader, the sensor captures power from the interrogating signal. A portion of the power received by the patch antenna at the sensor side is transferred to the RFID chip (SL3ICS1002 model manufactured by NXP Semiconductor). If the power is higher than the turn-on power of the RFID chip, the chip is activated and sends a modulated signal back to the reader antenna. A Tagformance Lite reader unit [12] from Voyantic Ltd. is adopted in this research. The reader captures the interrogation power threshold at each frequency point, by gradually increasing the interrogation power till the RFID chip is activated. The resonance frequency is identified as the minimum point in the figure plotting interrogation power threshold against frequency [10]. When the antenna deforms under strain, the antenna length is changed and thus the resonance frequency shifts accordingly. If a half-wave rectangular patch antenna were adopted in the sensor design, the antenna resonance frequency is related to patch length as:

$$f_0^{\text{Patch}} = \frac{c}{2(L+L')\sqrt{\varepsilon_{\text{reff}}}} \qquad (1)$$

where c is the speed of the light, L is the physical length of the antenna copper cladding (as metallic conductor of the antenna), $\varepsilon_{\text{reff}}$ is the effective dielectric constant of the substrate, and L' is the additional electrical length due to fringing effect. When the antenna is under strain, the shifted resonance frequency becomes:

$$f^{\text{Patch}} = \frac{c}{2(1+\varepsilon)(L+L')\sqrt{\varepsilon_{\text{reff}}}} = \frac{f_0^{\text{Patch}}}{1+\varepsilon} \approx f_0^{\text{Patch}}(1-\varepsilon) \qquad (2)$$

Eq. (2) shows that when strain ε is a small number, the relationship between the shifted resonance frequency and strain is approximately linear. In addition, when an antenna sensor is under compressive strain, the resonance frequency increases linearly. This linear relationship indicates strain can be derived by measuring shift in the antenna resonance frequency.

2.2 Folded patch antenna sensor design

If a 900MHz regular patch antenna sensor is designed, according to Eq. (1), the antenna length needs to be over 130mm. To reduce the sensor size, a folded path antenna sensor detours the surface current path by vias, which go through substrate and connect top copper cladding with bottom copper ground to increase electrical length travelled by the current. As a result, the folded patch antenna configuration can reduce antenna footprint by half, to 61mm × 69mm (Fig. 3). The substrate is made of 0.787mm-thick Rogers RT/duriod®5880 material, which has a low dielectric constant and a low loss tangent to improve interrogation distance and signal to noise ratio. Because of doubled current path produced by the antenna folding, the resonance frequency of the folded patch antenna sensor under strain is estimated as [11]:

$$f^{\text{Folded}} = \frac{c}{4(1+\varepsilon)(L+L')\sqrt{\varepsilon_{\text{reff}}}} = \frac{f_0^{\text{Folded}}}{1+\varepsilon} \approx f_0^{\text{Folded}}(1-\varepsilon) \qquad (3)$$

The relationship between the shifted frequency and strain is also approximately linear when strain is a small number.

2.3 Slotted patch antenna sensor design

Although a folded patch antenna design reduces sensor footprint, the size of the antenna sensor is still relatively large for localized strain measurement. To this end, a slotted patch antenna design can offer further size reduction. In a slotted patch antenna, vias are kept to maintain the benefit of antenna folding. Two slots are added on the top copper cladding to further detour surface current path. Final design of the slotted patch antenna has a dimension of 44mm × 48mm (Fig. 4). The substrate material and thickness are the same as the folded patch antenna sensor. Owing to current detouring, the resonance frequency of the slotted patch antenna sensor under strain is estimated as [9]:

$$f^{\text{Slotted}} = \frac{c}{8(1+\varepsilon)(L+L')\sqrt{\varepsilon_{\text{reff}}}} = \frac{f_0^{\text{Slotted}}}{1+\varepsilon} \approx f_0^{\text{Slotted}}(1-\varepsilon) \tag{4}$$

Thus, the slotted patch can achieve additional size reduction compared to the folded patch antenna, while the antenna sensor retains similar resonance frequency around 900MHz for utilization of the RFID chip.

3. MULTI-PHYSICS COUPLED SIMULATION FOR COMPRESSIVE STRAIN SENSING

Numerical simulation is conducted to evaluate compressive strain sensing performance of the folded patch and slotted patch antenna designs. Coupling structural mechanics and electromagnetics, the simulation is conducted using a commercial multi-physics software package, COMSOL. Section 3.1 describes the simulation model and simulated sensing performance of the folded patch antenna sensor. Section 3.2 provides descriptions for the slotted patch antenna sensor.
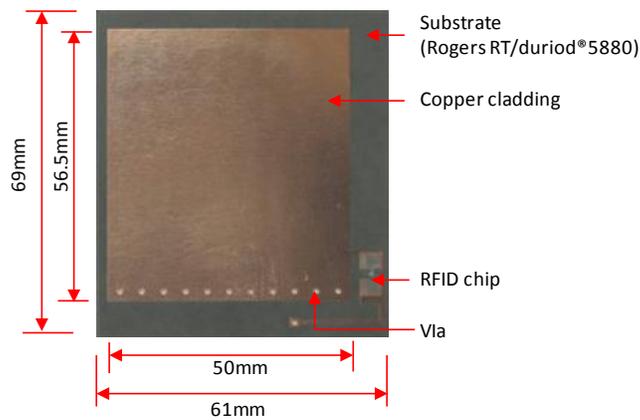

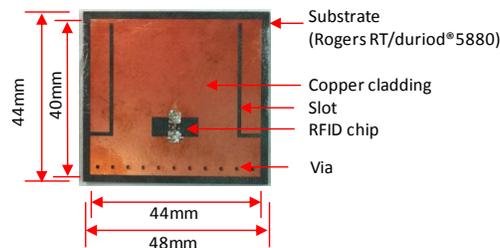Fig. 3. Folded patch antenna sensor with passive RFID chip

Fig. 4. Slotted patch antenna sensor with passive RFID chip

3.1 Mechanical and electromagnetic simulation of the folded patch antenna sensor

Fig. 5 presents the mechanics-electromagnetics coupled simulation model for the folded patch antenna sensor mounted on the tapered aluminum testing specimen. The air sphere delineates the electromagnetic domain. Because a larger air sphere requires longer simulation time, longitudinal dimension of the specimen is reduced. The slight reduction to tapered ends has little effect on the uniform compressive strain distribution. The outer surface of the air sphere is a perfectly matched layer (PML) which attempts to absorb radiation from the antenna and reflects no power back. The RFID chip (NXP Semiconductor) is modeled by a lumped port with an impedance of $13.3 - j122\Omega$. Tetrahedral and prism elements are adopted to model solid structures such as the aluminum specimen, substrate, and PML layer, and to efficiently resolve boundary layers. For modeling shell structures, such as top and bottom copper cladding, triangular elements are used to reduce discretization error and quadrilateral elements are adopted to achieve better numerical accuracy. Table 1 lists the number of each type of element, and the number of DOFs in COMSOL model.

To investigate strain sensing performance, multiple strain levels are applied to the folded antenna sensor, ranging from zero to -300µε with 50µε strain change per step. For the simulation coupling mechanics and electromagnetics, moving mesh technique is adopted so that the same finite element model can be used for simulating different physics. Specifically, the deformation of the antenna sensor under strain, which conforms to material mechanical properties and boundary conditions, is first solved using COMSOL mechanics module. The deformed mesh computed from mechanical domain is then directly transported to electromagnetic domain for simulating antenna radiation.

To evaluate the strain sensing performance of an antenna sensor, resonance frequency shift needs to be identified for each strain step. Because scattering parameter (S_{11}) represents antenna radiation efficiency at certain electromagnetic frequency, S_{11} is simulated to identify resonance frequency shift. The parameter, which shows the lowest magnitude at resonance frequency, is calculated as [13]:

$$S_{11} = \frac{V_{\text{out}}}{V_{\text{in}}}$$

(5)

where V_{in} and V_{out} are input (incident) and output (reflected) voltage at the lumped port (modeling RFID chip), looking into the antenna. If output (reflected) voltage is small at certain frequency, the antenna radiates more energy out, meaning the antenna has higher radiation efficiency at that frequency. Therefore, the frequency corresponding to minimum value of $|S_{11}|$ is regarded as the resonance frequency of the antenna. Because of fabrication and installation tolerance in practice, the resonance frequency at zero strain can be slightly different for each installed sensor. To accommodate the tolerance, the concept of normalized resonance frequency change, Δf_{N}, is introduced:

$$\Delta f_{\text{N}} = \frac{f_{\text{R}} - f_{\text{R0}}}{f_{\text{R0}}}$$

(6)

where f_{R0} is the resonance frequency at zero strain; f_{R} is the changed resonance frequency under strain ε. According to Eq. (3) or (4), the magnitude of Δf_{N} should be approximately equal to the magnitude of strain ε. However, in practice Δf_{N} has a smaller magnitude due to possible dielectric constant change of the substrate material under strain. The frequency change can also be affected by the strain transfer effect from specimen (structural) surface to top copper cladding of the antenna sensor. To consider these effects, the normalized strain sensitivity is estimated as follows:

$$\Delta f_{\text{N}} = -S_{\text{N}}\varepsilon$$

(7)

Table 1. Number of elements and degrees of freedom in the folded patch antenna sensor model

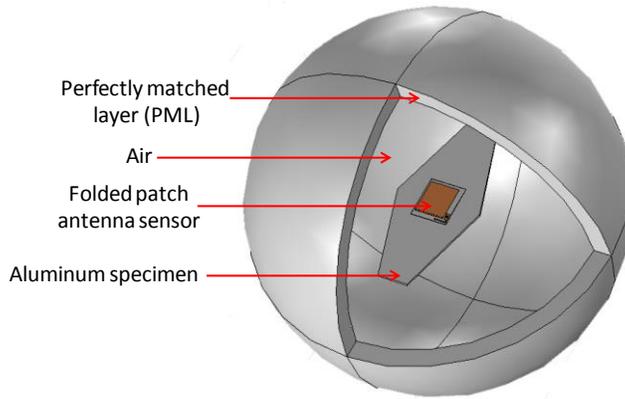| Number of Elements		Number of DOFs	
Tetrahedron	129,995	Mechanics	114,597
Prism	7,692		
Triangle	16,462	Electromagnetics	931,582
Quadrilateral	504		

Fig. 5. Multi-physics simulation model for the folded patch antenna sensor in COMSOL

where S_N is the normalized strain sensitivity, which is usually close to but lower than 1ppm/με (ppm - part per million) [11].

To illustrate simulated resonance frequency change of the antenna due to strain, Fig. 6(a) plots S_{11} parameter against frequency, at four different strain levels. The resonance frequency clearly shifts towards right as compressive strain increases. The resonance frequency at each strain level is extracted from S_{11} plot, and the normalized frequency change is calculated by Eq. (6) and plotted against strain in Fig. 6(b). Through linear regression to the data points of normalized frequency change versus strain, the coefficient of determination in Fig. 6(b) is found to be 0.9999, which as expected shows a highly linear relationship. To quantify strain measurement accuracy, the standard deviation (STD) error of the measurement is calculated as:
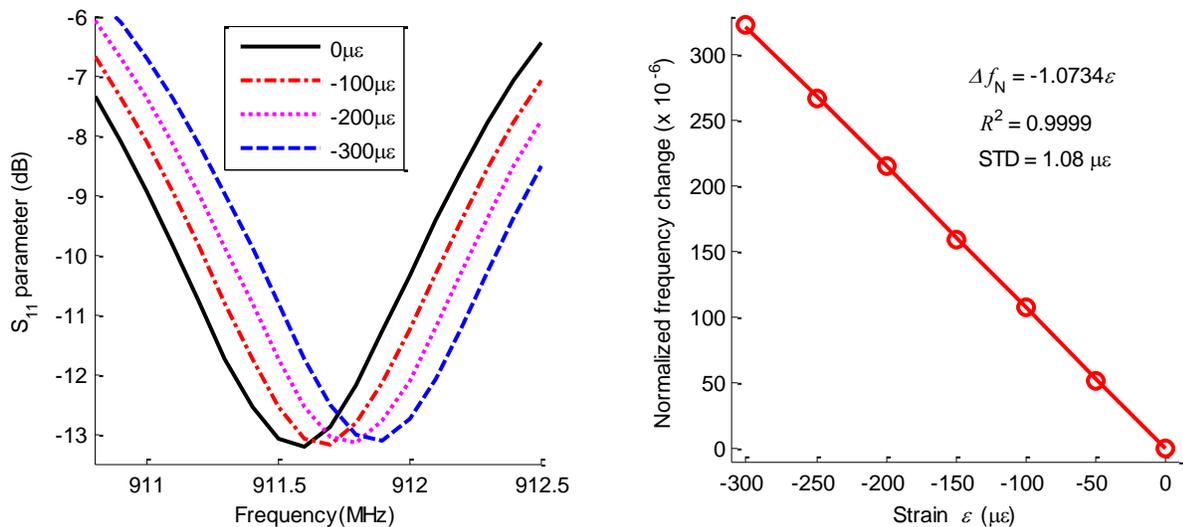
(a) Simulated S_{11} parameter at different strain level

(b) Normalized resonance frequency change versus strain ε

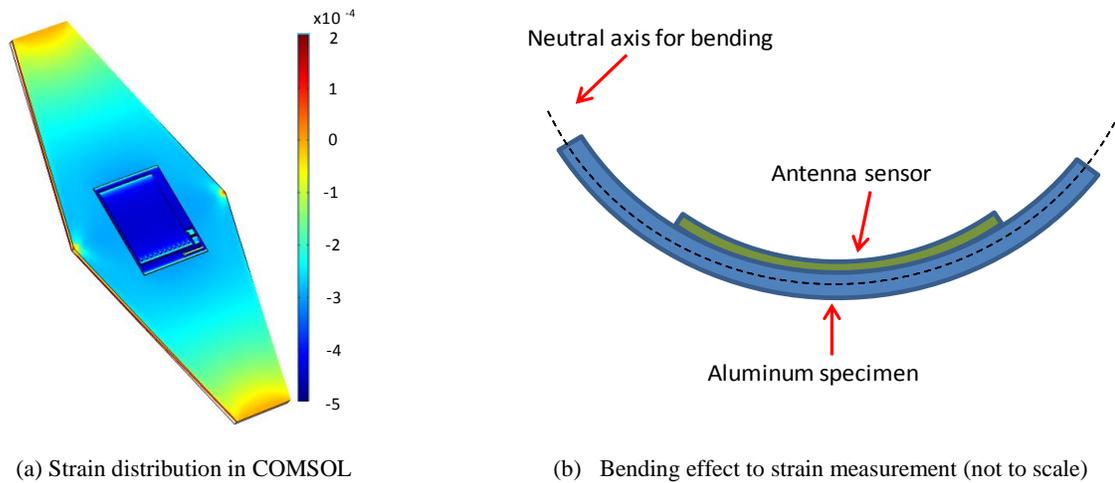Fig. 6. Strain simulation results of the folded patch antenna sensor in COMSOL

(a) Strain distribution in COMSOL   (b)   Bending effect to strain measurement (not to scale)

Fig. 7. Compression strain caused by bending

$$STD = \sqrt{\frac{\sum_{i=1}^{N}(\Delta \varepsilon_i)^2}{N-1}} \tag{8}$$

An each data point, $\Delta \varepsilon_i$ is the difference between the actual strain and strain value estimated from linear regression results; N is the total number of data points. The seven data points in Fig. 6(b) show a low STD value of 1.08με.

In addition, Fig. 6(b) shows the normalized strain sensing sensitivity, S_N, has a magnitude of 1.0734ppm/με. This is different from previous observation made when sensor is under tension, where S_N always has a magnitude less than 1.0 [11]. This difference can be explained by the three-point bending setup that generates the compression strain. Fig. 7(a) presents strain distribution of the folded patch antenna sensor and aluminum specimen generated by mechanical simulation. If the specimen is under pure tension without any bending, tensile strain on top copper cladding of the antenna is always lower than the surface strain of the specimen, due to strain transfer effect. However, in this study compressive strain on the antenna (around –400με) is distinguishably higher than that on the specimen (–300με). Fig. 7(b) attempts to explain this phenomenon caused by bending. When the antenna sensor is bent with the aluminum specimen, the distance from neutral axis to antenna top surface is longer than that to the aluminum specimen surface, which implies that strain on the antenna sensor surface is higher than that on the aluminum specimen. The simulation shows that when estimating strain from resonance frequency change, bending effect needs to be taken into consideration.

3.2 Mechanical and electromagnetic simulation of the slotted patch antenna sensor

Similar to the folded patch antenna described in Section 3.1, a COMSOL simulation model is constructed for the slotted patch antenna sensor. Table 2 summarizes the number of different elements and the number of DOFs. Because the slotted patch antenna has a smaller size than the folded patch, the corresponding element and DOF numbers are generally lower. Fig. 8(a) shows S_{11} plot under different strain level, and Fig. 8(b) plots the normalized frequency change against strain. The normalized strain sensitivity S_N is found to be –1.0366ppm/με. The coefficient of determination and STD error are 0.9994 and 2.64με, respectively. Compared to the folded patch antenna sensor, although the linearity between resonance frequency change and strain is slightly lower and STD error is higher, the results are still reasonable.

Table 2. Number of elements and degrees of freedom in the slotted patch antenna sensor model

Number of Elements		Number of DOFs	
Tetrahedron	46,954	Mechanics	59,487
Prism	6,596		
Triangle	440	Electromagnetics	348,374
Quadrilateral	815		

(a) Simulated S_{11} parameter at different strain level   (b) Normalized resonance frequency change versus strain ε
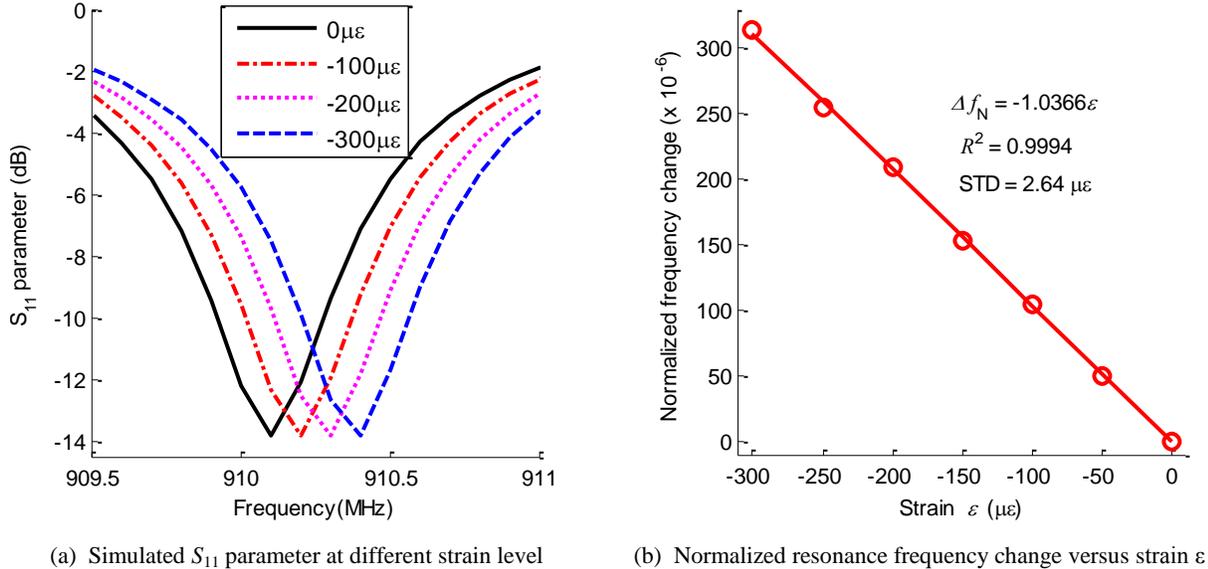
Fig. 8. Strain simulation results of the folded patch antenna sensor in COMSOL

4. EXPERIMENTAL RESULTS FOR FOLDED PATCH ANTENNA SENSOR AND SLOTTED PATCH ANTENNA SENSOR

Compression tests are conducted to experimentally investigate the compressive wireless strain sensing performance of the two antenna sensors. Section 4.1 describes experimental setup and results for the folded patch. Section 4.2 presents the experimental results for the slotted patch antenna sensor.

4.1 Compressive strain sensing test for folded patch antenna sensor

Wireless compressive strain sensing test is conducted to evaluate the performance of the folded patch antenna sensor (Fig. 9). Using the three-point bending setup, compressive strain is generated from zero to –300με, at an increment of –50με per step. The antenna sensor and reference metal foil strain gages are installed in the middle of tapered aluminum specimen. A National Instruments strain gage module is used for data collection from strain gages. The interrogation distance between the antenna sensor and Yagi reader antenna is set as 36 in. The interrogation power threshold is measured by a Tagformance RFID reader at each strain step (Fig. 9). The average interrogation power threshold plots are shown in Fig. 10(a). Only four strain levels are plotted for clarity. The strain values shown in the legend (0με, –106με, –201με, and –307με) are average readings from strain gages. Fig. 10(b) plots the normalized frequency change with strain. The normalized strain sensitivity is –0.9215ppm/με, which has a lower magnitude than simulation result. The coefficient of determination is 0.9980, showing high linearity. The approximately linear relationship between frequency change and strain, as predicted by Eq. (2), is thus experimentally confirmed. The STD error is 4.82με, which as expected is higher than simulation due to environmental electromagnetic noise.

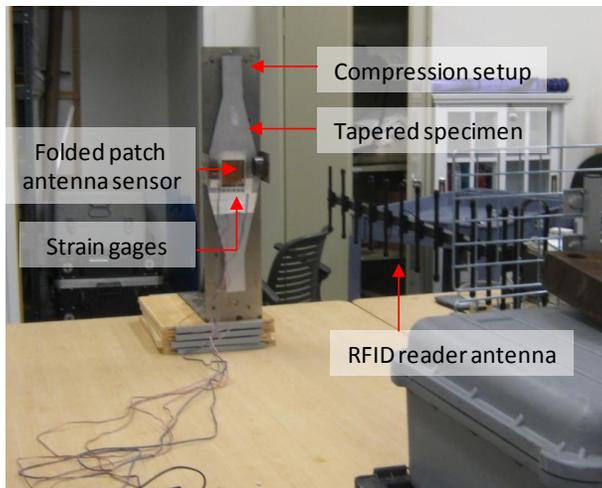Fig. 9. Experimental setup for compressive test with the folded patch antenna sensor
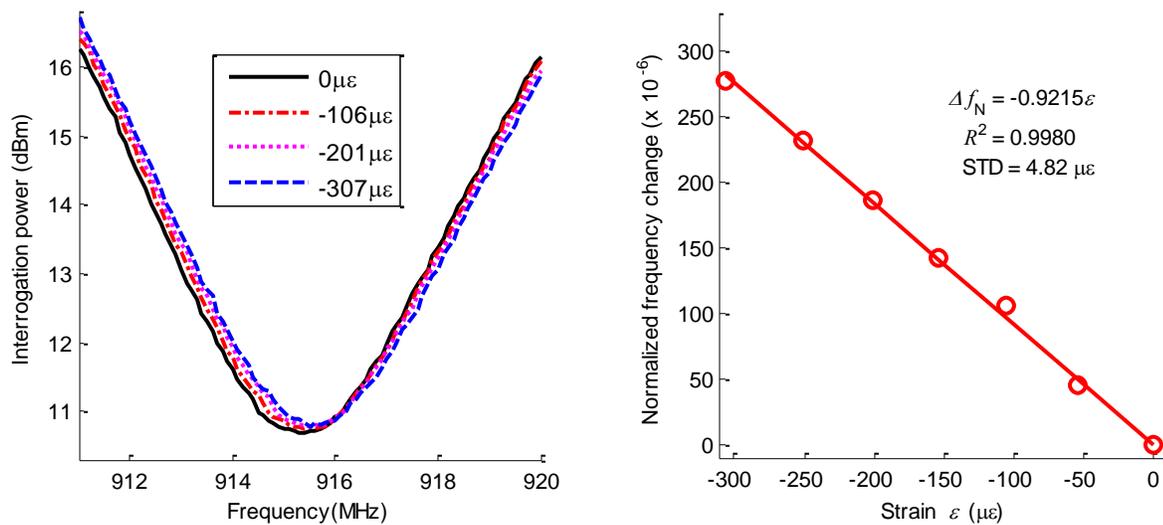

(a) Average interrogation power threshold

(b) Resonance frequency change with strain ε

Fig. 10. Compressive strain sensing test for the passive folded patch antenna sensor (strain increment: -50με)

4.2 Compressive strain sensing test for slotted patch antenna sensor

Using similar experimental setup and procedure, compression test for the slotted patch antenna sensor is conducted. Fig. 11(a) presents the average interrogation power threshold and Fig. 11(b) plots the normalized resonance frequency versus strain. The normalized strain sensitivity is –0.8706ppm/με, which is lower than the folded patch antenna sensor. As described in Section 3, the simulation results also show that the slotted patch antenna sensor has slightly lower sensitivity. The coefficient of determination is 0.9967, which indicates a fairy linear relationship between frequency change and strain. The STD error, 6.72με, is higher than the folded patch antenna sensor, but can still be acceptable for many applications.

5. SUMMARY AND CONCLUSION

This research presents the performance of compressive strain sensing for two wireless RFID antenna sensors. Compressive strain effects are first evaluated by mechanics-electromagnetics coupled simulation, using COMSOL multi-
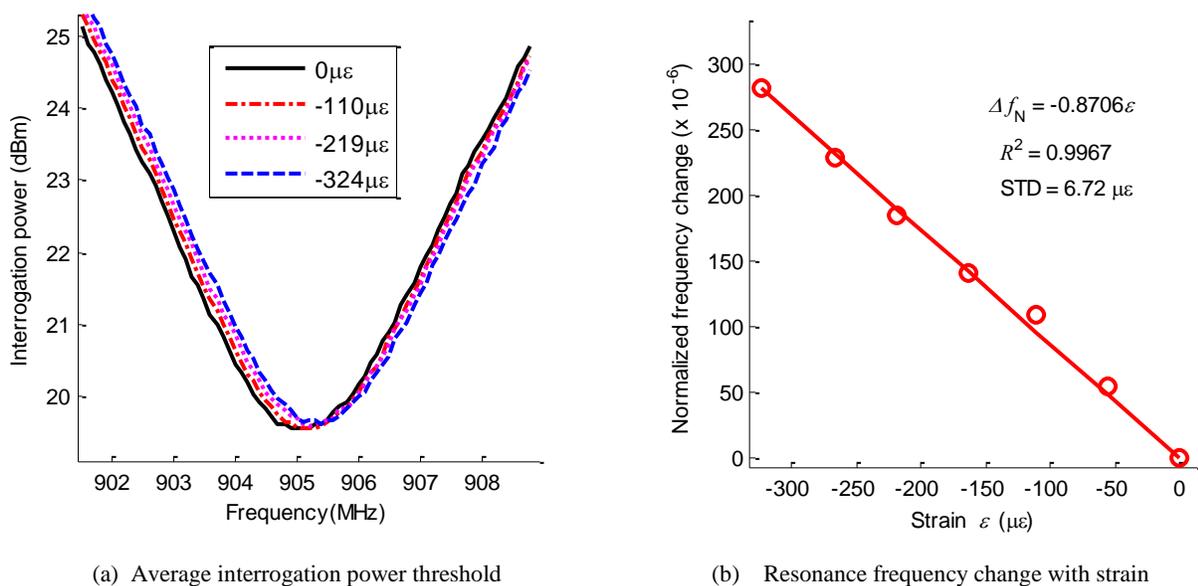
(a) Average interrogation power threshold   (b) Resonance frequency change with strain

Fig. 11. Compressive strain sensing test for the passive slotted patch antenna sensor (strain increment: -50με)

physics software package. To experimentally verify the performance, compressive strain measurements are conducted using a three-point bending setup. The size of the slotted patch antenna sensor is reduced to half of the folded patch antenna sensor, while the slotted patch sensor still provides reasonable accuracy. In the future, more extensive compression tests will be conducted to identify performance indexes such as sensitivity consistency and interrogation distance limit.

6. ACKNOWLEDGMENT

REFERENCES

[1]   Sohn, H., Farrar, C. R., Hemez, F. M., Shunk, D. D., Stinemates, D. W. and Nadler, B. R., [A Review of Structural Health Monitoring Literature: 1996-2001], Report No. LA-13976-MS, Los Alamos National Laboratory, Los Alamos, NM, USA (2003).

[2]   Zhou, Y., So, R. M. C., Jin, W., Xu, H. G. and Chan, P. K. C., "Dynamic strain measurements of a circular cylinder in a cross flow using a fibre bragg grating sensor," Experiments in Fluids, 27(4), 359-367 (1999).

[3]   Sirohi J, C. I., "Fundamental Understanding of Piezoelectric Strain Sensors," Journal of Intelligent Material Systems and Structures, 11, 246-257 (2000).

[4]   Çelebi, M., [Seismic Instrumentation of Buildings (with Emphasis on Federal Buildings)], Report No. 0-7460-68170, United States Geological Survey, Menlo Park, CA, USA (2002).

[5]   Straser, E. G. and Kiremidjian, A. S., [A Modular, Wireless Damage Monitoring System for Structures], Report No. 128, John A. Blume Earthquake Eng. Ctr., Stanford University, Stanford, CA, USA (1998).

[6]   Wang, Y., Lynch, J. P. and Law, K. H., "A wireless structural health monitoring system with multithreaded sensing devices: design and validation," Structure and Infrastructure Engineering, 3(2), 103-120 (2007).

[7]   Lynch, J. P. and Loh, K. J., "A summary review of wireless sensors and sensor networks for structural health monitoring," The Shock and Vibration Digest, 38(2), 91-128 (2006).

[8]   Yi, X., Wu, T., Lantz, G., Cooper, J., Cho, C., Wang, Y., Tentzeris, M. M. and Leon, R. T., "Sensing resolution and measurement range of a passive wireless strain sensor," Proceedings of the 8th International Workshop on Structural Health Monitoring (IWSHM) (2011).

[9]   Yi, X., Wang, Y., Tentzeris, M. M. and Leon, R. T., "Multi-physics modeling and simulation of a slotted patch antenna for wireless strain sensing," Proceedings of the 9th International Workshop on Structural Health Monitoring (IWSHM) (2013).

[10]   Yi, X., Wu, T., Wang, Y., Leon, R. T., Tentzeris, M. M. and Lantz, G., "Passive wireless smart-skin sensor using RFID-based folded patch antennas," International Journal of Smart and Nano Materials, 2(1), 22-38 (2011).

[11]   Yi, X., Cho, C., Cooper, J., Wang, Y., Tentzeris, M. M. and Leon, R. T., "Passive wireless antenna sensor for strain and crack sensing-electromagnetic modeling, simulation, and testing," Smart Materials and Structures, 22(8), 085009 (2013).

[12]   Voyantic, [Tagformance Lite Measurement System User Guide], Voyantic Ltd., Espoo, Finland (2011).

[13]   Pozar, D. M., [Microwave Engineering], Wiley & Sons, Inc., New York, NY, USA (2012).